J Acupunct Meridian Stud 2010;3(3):150–155

RESEARCH ARTICLE

ELSEVIER

Fluorescent Nanoparticles for Observing Primo Vascular System Along Sciatic Nerve

Zhao-Feng Jia[1,2], Byung-Cheon Lee[1,3]*, Ki-Hoon Eom[1], Jin-Myung Cha[4], Jin-Kyu Lee[4], Zhen-Dong Su[1,2], Wen-Hui Yu[2], Pan Dong Ryu[5], Kwang-Sup Soh[1]

[1]*Biomedical Physics Laboratory, Department of Physics and Astronomy, Seoul National University, Seoul, Korea*
[2]*Chinese Traditional Veterinary Laboratory, Department of Animal Medicine, Northeast Agriculture University, Harbin, China*
[3]*Pharmacopuncture Medical Research Center, Korean Pharmacopuncture Institute, Seoul, Korea*
[4]*Materials Chemistry Laboratory, Department of Chemistry, Seoul National University, Seoul, Korea*
[5]*Laboratory of Veterinary Pharmacology, College of Veterinary Medicine, Seoul National University, Seoul, Korea*

Received: Jun 29, 2010
Accepted: Jul 15, 2010

KEY WORDS:
acupuncture;
epineurium;
primo vascular system;
primo-vessel;
sciatic nerve;
Zusanli (ST-36)

Abstract
The primo vascular system was found in the epineurium along the rat sciatic nerve following subcutaneous injection of fluorescent nanoparticles at the Zusanli acupoint (ST-36). Nanoparticles were injected into the primo-vessel near ST-36 and flowed along the sciatic nerve. Fluorescence revealed a structure in the epineurium that was hardly detectable. Images of the isolated sample stained with 4',6-diamidino-2-phenylindole were captured using confocal microscopy. These images showed the distinctive nuclei distribution and multi-lumen structure of primo-vessels that differentiate them from lymphatic vessels, blood capillaries and nerves. This study demonstrates a new use for nanoparticles in fluorescence reflectance imaging techniques during *in vivo* imaging of primo-vessels.

1. Introduction

The primo vascular system (PVS) was first introduced as the anatomical structure of acupuncture meridians by Bonghan Kim [1], and was recently rediscovered by a group working at Seoul National University [2]. The PVS was distributed as an additional circulatory system to the cardiovascular and lymphatic system not only in the skin but also throughout the body, and most surprisingly, in the brain and the nervous system. The PVS has been detected in the brain ventricles and central canal of the spinal cord of rabbit using hematoxylin [3,4], and in the brain, spine, and sciatic nerve of rat by Trypan blue [5].

In these studies, however, the relationship between the acupuncture points and the nervous primo vascular system (NPVS) was not investigated. In the present work, we developed a new method, which is suggestive of a close relationship between a peripheral nerve and the NPVS. We injected fluorescent nanoparticles into the hypodermal layer at the Zusanli acupoint (ST-36) and observed their flow into the primo-vessel in the epineurium of

*Corresponding author. Biomedical Physics Laboratory for Korean Medicine, Department of Physics and Astronomy, Seoul National University, 599 Gwanak, Gwanak-gu, Seoul 151–747, Korea.
E-mail: donboscolee@gmail.com

the sciatic nerve. Nanoparticles injected at ST-36 flowed in the lymphatic vessel more often than in the primo-vessel, and it was necessary to discern the vessels by examining the distribution of the nuclei in these structures.

This study allowed the visualization of the PVS in the epineurium of the sciatic nerve. The flow of the PVS from the region around the acupoint ST-36, and the first use of fluorescent nanoparticles to observe the NPVS were also demonstrated in this work. Considering the close relationship between the peripheral nervous system and acupuncture treatment [6], studying the NPVS further to uncover its function with respect to the physiology of the sciatic nerve and acupuncture mechanisms may elucidate further knowledge regarding this treatment method.

2. Materials and Methods

2.1. Animals

Seven male Wistar rats (approximately 200 g) and three male Sprague-Dawley rats (approximately 200 g) were obtained from the Jung Ang Laboratory Animal Company (Seoul, Korea). The animals were housed in a constant temperature controlled environment (26°C) with 60% relative humidity. All animals were exposed to a 12-hour light-dark cycle and had *ad libitum* access to food and water. Procedures involving the animals and their care conformed to the institutional guidelines of Seoul National University, which were in full compliance with current laws and policies [7].

2.2. Fluorescent tracer solution

Cobalt-ferrite magnetic nanoparticles embedded with amorphous silica, which contained a fluorescent dye, rhodamine B isothiocyanate (RITC, orange, $\lambda_{max}=555$ nm) on the inside of a silica shell and biocompatible poly (ethylene glycol; PEG) on the outside of the silica shell, were synthesized. The average size of the fluorescent magnetic nanoparticles was approximately 9 nm while the total size of the core shell structure was around 50 nm. The concentration of particles was 10 mg/cm^3, which were suspended in a sterile saline solution at pH 7.4 [8,9].The fluorescent tracer solution was composed of the fluorescent magnetic nanoparticles and ≥99.9% ethyl alcohol (Sigma, St Louis, MO, USA) in a ratio of 1:1.

2.3. Injection of nanoparticles

The rats were anesthetized with urethane (1.5 g/kg) which was administered intramuscularly; all surgical procedures were performed under general anesthesia. Before injection the hair of the lower limb region was removed using clippers. Nanoparticles were injected into the classical acupuncture point of the lower limb, Zusanli (ST-36), which was located 3 cun below ST-35, one finger width lateral from the anterior border of the tibia. The injection needle (31-gauge syringe, 0.25 mm in diameter and 8 mm in length) was thinner than an acupuncture needle tip. The fluorescent tracer solution (0.06 mL for each ST-36) was injected subcutaneously, avoiding blood vessels to prevent bleeding.

2.4. Imaging

Four hours after the injection of nanoparticles, the lower limbs were dissected and the sciatic nerve was exposed. Fluorescence emission from nanoparticles was detected with a fluorescence microscope (MVX 10; Olympus Co., Tokyo, Japan) equipped with a sensitive black/white charged-coupled device camera and a long-pass filter (600 nm; CVI, Seoul, Korea) [10–12].

2.5. Confocal laser scanning microscope

The observation of small pieces of threadlike structures (500 μm–1 mm) beside the nerve, lymphatic vessel, or blood vessel was performed using an MVX10 microscope (Olympus Co.) and a phase contrast microscope (BX 51; Olympus Co). Confocal laser scanning microscope images were obtained (LSM 510; Carl Zeiss, Jena, Germany).

2.6. Histology

For histological studies, the threadlike structures in the epineurium of the sciatic nerve were fixed in 10% neutral buffered formalin over night. After 24 hours, the target sample was frozen and embedded in OCT compound, then 8 μm sections were cut with a freezing microtome and stained with a DAPI (4′,6-diamidino-2-phenylindole, SlowFade Gold; Invitrogen, Carlsbad, CA, USA) solution and DiO (3,3′-dioctadecyloxacarbocyanine, perchlorate). The sections were observed and photographed under a phase contrast microscope (BX 51; Olympus Co.).

3. Results

As shown in Table 1, we performed 12 experiments, among which eight positive results revealed primo-vessels along the sciatic nerves. Fluorescent nanoparticles injected into the hypodermis at the acupuncture ST-36 diffused and were absorbed by the lymph and primo-vessels. The primo-vessel along

Table 1 Nanoparticle flow in primo-vessels of rats

No.	Strain	Sex	Weight (g)	Flow of nanoparticles in primo-vessels (length of flow)
1	Wistar	M	235	Along epineuria (3 mm)①
2	Wistar	M	250	Along perineurium (2 mm)①
3	Wistar	M	190	X
4	Wistar	M	185	X
5	Wistar	M	170	Along epineuria (10 mm)②
6	Wistar	M	210	Along perineurium (1 mm)①
7	SpD	M	230	Along epineuria (2 mm)①
8	Wistar	M	200	Along epineuria (4 mm)③
9	Wistar	M	175	Along perineurium (6 mm)②
10	Wistar	M	220	X
11	SpD	F	190	X
12	SpD	F	240	Along epineuria (3 mm)③

SpD=Sprague-Dawley; X=not observed; M=male; F=female; ①,②,③,=primo-vessels where nanoparticles flowed along the three nerves as shown in Figure 1.

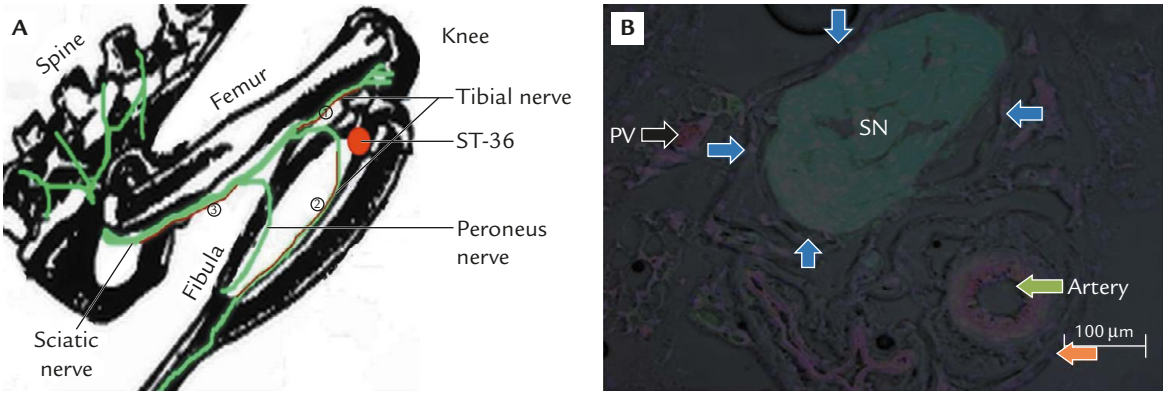

Figure 1 (A) Schematic illustration of the sciatic nerve (green line) of the lower limb, and primo-vessels (red colored curves) containing nanoparticles. The red spot represents the Zusanli acupoint (ST-36) into which nanoparticles were injected. ①,②,③ are the three separate regions where the nanoparticles were detected in the primo-vessels. (B) Cross-sectional image of the sciatic nerve with its associated primo-vessel indicated by a black arrow. Primo-vessel diameter was approximately 20 μm, and fluorescent nanoparticles were detected only if the primo-vessel was located in the epineurium. Blue arrows delineate the boundaries of the perineurium. An artery was present in the epineurium. The orange arrow indicates the boundary of the epineurium. PV=primo-vessel; SN=sciatic nerve.

the epineurium or perineurium of the sciatic nerve in the lower limb of rat was visualized using the fluorescence nanoparticles that flowed in the primo-vessel. Figure 1 illustrates the anatomical positions of the primo-vessels with respect to the epineurium and perineurium of the sciatic nerve.

In Figure 2, a primo-node and two branches of primo-vessels in the epineurium of the tibial branch of the sciatic nerve were detected by using a fluorescence microscope to observe the fluorescence of the nanoparticles. The sample was taken from area numbered 2 in Figure 1. Lymph vessels were frequently observed, as shown in Figure 2B; it was possible to distinguish the primo-vessel from lymph vessels by comparing the distributions and shapes of nuclei in the vessels, as shown in the right upper panels [13].

Confocal laser scanning microscopic images of the primo-vessels along the common peroneal nerve are shown in Figure 3. The lower panels are magnified views of the rectangular areas shown in the corresponding upper three panels. The fluorescence of the nanoparticles that flowed in the primo-vessel, clearly demonstrated that the nanoparticles flowed only in the primo-vessel and not in neighboring tissues (Figure 3A). The distribution of nuclei in the primo-vessel was clearly different to that of neighboring tissues (Figure 3B); however, the presence of the primo-vessel is barely detectable using phase contrast imaging (Figure 3C). When images were merged, the characteristic distribution of nuclei and the flowing path of nanoparticles coincided (Figure 3D).

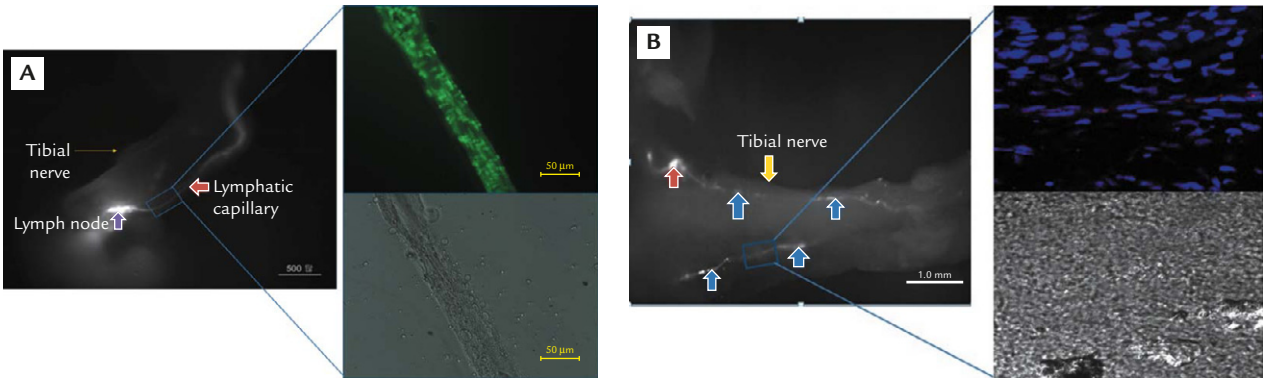

Figure 2 (A) Fluorescence image of a section of the tibial nerve (in Figure 1A) fixed with 10% neutral buffered formalin. The lymphatic capillary and node are bright due to fluorescent nanoparticles. The nuclei are transverse to the lymph vessel, as revealed by acridine orange staining (right upper panel). A phase contrast image of the isolated lymph vessel is shown in the right lower panel. (B) Fluorescence image of a section of the tibial nerve (in Figure 1A) fixed with 10% neutral buffered formalin. The primo-vessels (blue arrows) and primo-node (red arrow), located in the epineurium of the tibial nerve, are bright due to fluorescent nanoparticles. 4′,6-Diamidino-2-phenylindole staining revealed that the direction of the rod-shaped nuclei (overlapped with red nanoparticle signal) was along the primo-vessel and aligned in broken lines (right upper panel). A phase contrast image of the primo-vessel with the peroneal nerve in the background is shown in the right lower panel.

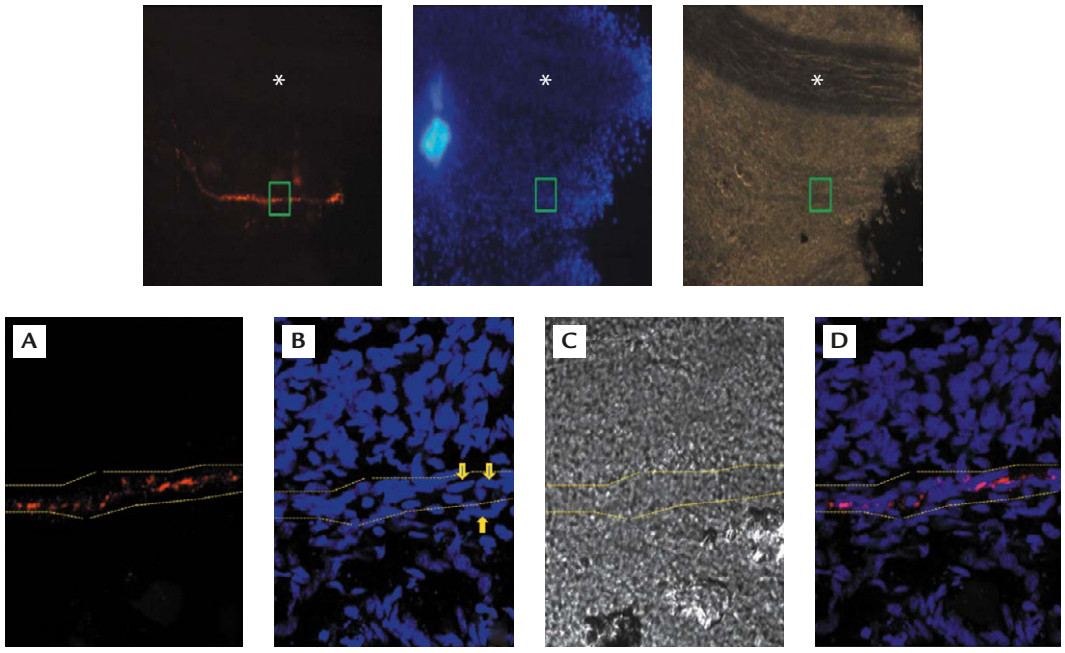

Figure 3 Confocal laser scanning microscopy of the primo-vessels along the common peroneal nerve (asterisks). (A) Signals of nanoparticles. (B) 4′,6-diamidino-2-phenylindole image. (C) Phase contrast image. (D) Merged image of A and B. The nanoparticles (red) flowed only in the primo-vessels (diameter 20 μm) in the perineurium. The shape and the distribution of the nuclei (yellow arrow) in the primo-vessel are different from neighboring tissues. They are longitudinally arranged along the primo-vessel. The primo-vessel (between the yellow dotted lines) was barely discernible from neighboring tissues in phase contrast images. The lower panels are magnified views of the rectangular areas indicated in images above them. Upper panels, 100×; lower panels, 600× taken using a confocal laser scanning microscope.

Cross sections of the tibial nerve and a primo-vessel were obtained using cryo-sectioning and were examined after DAPI and DiO staining. As shown in Figure 4, the phase contrast images of the nerve and the primo-vessels explicitly showed that the primo-vessel was located in the epineurium and had two channels. The DAPI images showed the presence of nuclei in the primo-vessel while the DiO images showed the presence of a membrane. The last panel demonstrates the presence of nanoparticles in the primo-vessel channels. These images manifestly demonstrate that the nanoparticles

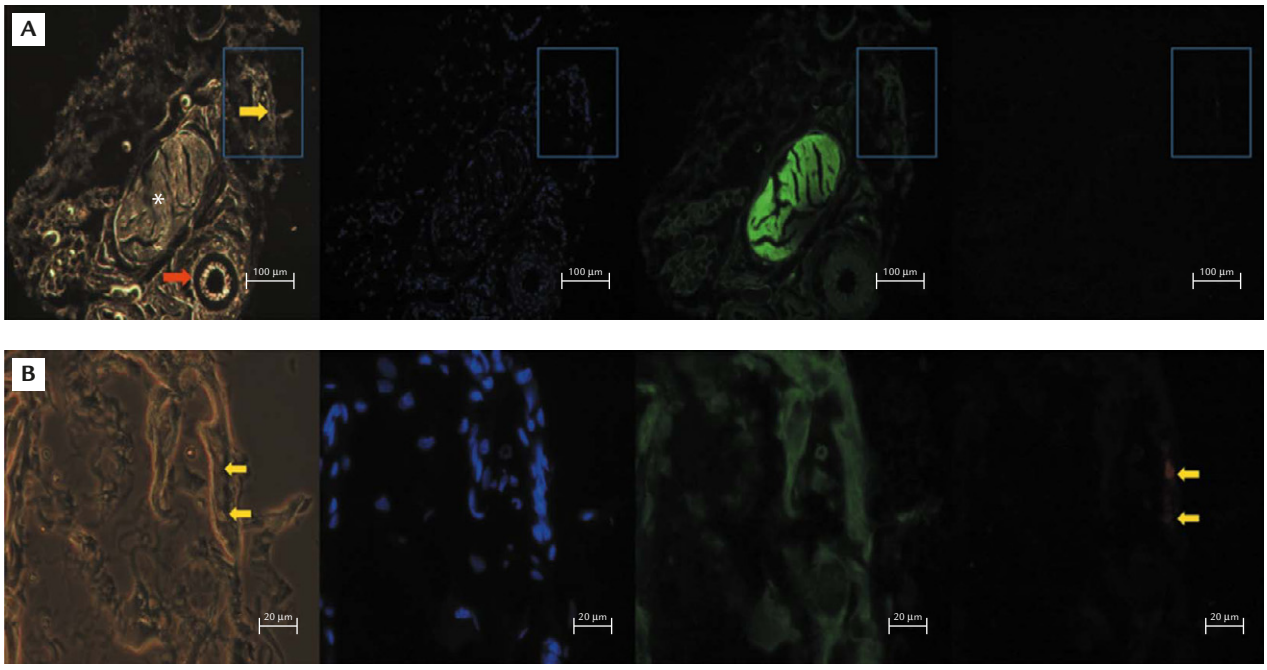

Figure 4 Cross-sectional images of a cryo-sectioned tibial nerve (asterisk) with its associated blood vessel (red arrow) and primo-vessel (yellow color) in the surrounding epineurium. DAPI (blue) showed the distribution of nuclei, and the 3,3′-dioctadecyloxacarbocyanine DiO image revealed membrane as well as nerve structure. The last panel shows only the fluorescence of the nanoparticles. The lower panels (400×) are higher magnifications of the rectangular areas indicated in the upper panel (100×). The fluorescent nanoparticles flowed in the primo-vessel, which had two channels (yellow arrows). The diameter of these channels was approximately 5 μm while the length of the long and short primo-vessels was 30 μm and 10 μm, respectively. The short primo-vessel was squeezed or obliquely sectioned in the histological process.

flow only in the primo-vessel through two channels, but not in the other parts of the nerve.

4. Discussion

The therapeutic effects and electrical properties of ST-36, one of the most well known acupoints, have been extensively studied. Electrical stimulation at this acupoint for hypertension has been especially important in the scientific investigation of the influence that ST-36 has on the nervous system [6]. With respect to anatomical aspects, Bonghan Kim [1] claimed that a PVS at the ST-36 ran along the sciatic nerve toward the spine. However, he did not describe his methods or his results, either in figures or words; thus, his findings have yet to be reproduced.

In the present experiment we injected fluorescent nanoparticles at ST-36 of a rat and found the PVS in the epineurium, running along the sciatic nerve. The PVS could be traced to just slightly beyond the area of diffusion of the nanoparticles, not to ST-36. Some of the diffused nanoparticles did somehow get into the PVS and flowed toward the spine. They did not flow in other areas of the epineurium or in the sciatic nerve. Nanoparticles were more frequently observed in the lymph vessels than in the primo-vessels. Therefore, it was critical to discern the PVS from the lymph system. Our previous works helped us resolve this problem, as we found that the distributions of nuclei in the lymph and primo-vessels were characteristically different [2]. Lymph vessel nuclei are predominantly transverse to the direction of the vessel whereas primo-vessel nuclei are mostly longitudinal to the primo-vessel direction, as depicted in Figures 2A and 2B. Another characteristic feature of primo-vessels, compared to blood or lymph vessels, is their multi-channel nature constructed from extracellular matrices of collagen fibers (Figure 4).

The primo-vessel is extremely difficult to identify using an ordinary histological staining method, such as hematoxylin and eosin (H&E), as the vessel is mostly composed of a thin membrane and small lumens. The membranes are composed of collagen fibers, which are also the main components of the surrounding connective tissues, thus further increasing the difficulty of observing these structures using H&E. In our case, we were able to identify the primo-vessel by the flow of fluorescence nanoparticles. In future studies, however, one will be able to recognize the PVS in the epineurium by using only a suitable histological technique, without the

flowing visualizing agents, as this work has established the detailed histological characteristics of the PVS.

We cannot explain, however, the mechanism by which nanoparticles entered the PVS near ST-36, nor could we trace them back to ST-36. This may be possible in the future using a more refined histological identification method. Kim [1] speculated that the PVS provided nutrients to keep the nervous system healthy, allowing regeneration when the nervous system was in disorder. However, Kim's idea may require further investigation.

Acknowledgments

This work was supported by a grant (No. R01-2008-000-11602-0) from the Mid-career Researcher Program of NRF funded by the Korean Government (MEST). K. Soh and Z. Jia thank the Association of Korean Oriental Medicine for its financial support.

References

1. Kim BH. On the Kyungrak System. *J Acad Med Sci DPR Korea* 1963;90:1–41.
2. Soh KS. Bonghan circulatory system as an extension of acupuncture meridians. *J Acupunct Meridian Stud* 2009;2: 93–106.
3. Lee BC, Kim S, Soh KS. Novel anatomic structures in the brain and spinal cord of rabbit that may belong to the Bonghan system of potential acupuncture meridians. *J Acupunct Meridian Stud* 2008;1:29–35.
4. Lee BC, Kim KW, Soh KS. Characteristic features of a nerve primo-vessel suspended in rabbit brain ventricle and central canal. *J Acupunct Meridian Stud* 2010;3:75–80.
5. Lee BC, Eom KH, Soh KS. Primo-vessels and primo-nodes in rat brain, spine and sciatic nerve. *J Acupunct Meridian Stud* 2010;3:111–5.
6. Tjen-A-Looi SC, Li P, Longhurst JC. Medullary substrate and differential cardiovascular responses during stimulation of specific acupoints. *Am J Physiol Regul Integr Comp Physiol* 2004;287:R852–62.
7. Institute of Laboratory Animal Resources Commission on Life Sciences. *Guide for the Care and Use of Laboratory Animals*. Washington: National Academy Press, 1996.
8. Yoon TJ, Kim JS, Kim BG, Yu KN, Cho MH, Lee JK. Multifunctional nanoparticles possessing a "magnetic motor effect" for drug or gene delivery. *Angew Chem Int Ed Engl* 2005;44:1068–71.
9. Lee C, Yoo JS, Kwon J, Soh KS. Study on the flow through the organ surface Bonghan duct by using nanoparticles. *J Korean Soc Jungshin Sci* 2006;10:49–55.
10. Lee BC, Yoo JS, Ogay V, Kim KW, Dobberstein H, Soh KS, et al. Electron microscopic study of novel threadlike structure on the surfaces of mammalian organs. *Microsc Res Tech* 2007;70:34–43.
11. Lee BC, Yoo JS, Baik KY, Sung B, Lee J, Soh KS. Development of fluorescence stereomicroscope and observation of Bong-Han corpuscles inside blood vessels. *Indian J Exp Biol* 2008; 46:330–5.
12. Yoo JS, Johng HM, Yoon TJ, Shin HS, Lee BC, Lee C, et al. In vivo fluorescence imaging of threadlike tissues (Bonghan ducts) inside lymphatic vessels with nanoparticles. *Curr Appl Phys* 2007;7:342–8.
13. Ogay V, Bae KH, Kim KW, Soh KS. Comparison of the characteristic features of Bonghan ducts, blood and lymphatic capillaries. *J Acupunct Meridian Stud* 2009;2:107–17.